

# **Quantum interference depression in thin metal films with ridged surface**

Avto N. Tavkhelidze\*, Amiran Bibilashvili and Larissa Jangidze  
*Tbilisi State University, Chavchavadze Avenue 13, 0179 Tbilisi, Georgia*

Brian Bilenberg  
*NIL Technology Oersted's Plads DTU Building 347 DK-2800 Kongens Lyngby  
Denmark*

Hans Walitzki  
*Avto Metals plc, London, England, United Kingdom NW3 7TS*

Martin E. Kordesch  
*Clippinger 158, Department of Physics, Ohio University, Athens, Ohio 45701-2979*

Changes in the metal properties caused by periodic indents in the metal surface were studied. It was shown that, ridged geometry of the wall leads to Quantum Interference Depression (QID), or reduction of the density of quantum states for the free electron. Wave-vector density in  $k$  space is reduced within the entire Fermi sphere. At the same time the number of electrons does not change, as the metal remains electrically neutral. Because of the Pauli Exclusion Principle, some electrons must occupy quantum states with higher wave numbers. The Fermi vector and Fermi energy of low-dimensional metal increase, and consequently, its work function decreases. In the experiment, irregularities such as granular structure of the film and the roughness of the surface reduce QID degree. Grain boundaries inside the film and surface roughness cause de Broglie wave scattering and reduce QID waveband. Recent experiments demonstrated a reduction of work function in thin films of Au, Nb, Cr and SiO<sub>2</sub>. Experimental results are in good qualitative agreement with the theory.

73.22.-f

## Introduction

Thanks to recent development of nanoelectronics, devices such as resonant tunneling diodes and transistors, super-lattices, quantum wells, and others, based on wave properties of electrons are fabricated <sup>1</sup>. Under certain conditions an electron in a solid can be regarded as a planar wave. The main requirement is that at least one dimension of the solid should be less than the mean free path of the electron. In this case, the electron can move without scattering and could be regarded as de Broglie wave. Transport properties of solids such as current and heat transport are defined by electrons having energies close to the Fermi level, and the mean free path is given for those electrons. Other free electrons inside solids, for example, ones having energies below Fermi level, do not participate in current and heat transport, because it is quantum mechanically forbidden for them to exchange energy with the environment, and hence the mean free path of such electrons is formally infinite. Such electrons will remain ballistic inside relatively large structures. In this work we use wave properties of such electrons to change the electronic structure of a solid. We analyze what happens when regular indents, which cause interference of de Broglie waves, are fabricated on the surface of a thin metal film. We will study the free electrons inside a rectangular potential-energy box with indented wall. We have shown that modifying the wall of a rectangular potential-energy box leads to a Quantum Interference Depression (QID), or reduction of the density of quantum states for the electron <sup>2</sup>. The Fermi vector and Fermi energy of low-dimensional metal increase, and consequently, its work function decreases. Results obtained for the potential-energy box were extrapolated to the case of low-dimensional metals (thin metal films). The influence of irregularities of thin metal films, such as the grains inside the film and the roughness of surface of the film, was studied. Thin metal films of Au and Cr were

grown using exploding wire evaporation and quench condensing both at cooled and room temperature substrates. E-beam evaporation method was used for Nb and Au films. Work function reduction was measured in Au, Nb, Cr and SiO<sub>2</sub> thin films. Experimental results were interpreted as limitation of QID effect by irregularities of the film.

In this work we use wave properties of ballistic electrons to change the electronic structure of a solid in the way that the work function of the solid could be reduced and regulated. Such materials will find many applications in devices based on electron emission and electron tunneling, and in semiconductor industry.

### **Calculation of Fermi energy based on volume perturbation method**

Assume a rectangular potential-energy box, with one of the walls modified as shown in Fig.1. The indents on the wall have the shape of strips of depth of  $a$  and width  $w$ . We name the box shown on Fig.1 as Ridged Potential-Energy Box (RPEB) to distinguish it from the ordinary Potential-Energy Box (PEB). The time-independent Schrödinger equation for an electron wave function inside the RPEB can be rewritten in the form of Helmholtz equation

$$(\nabla^2 + k^2) \Psi = 0, \quad (1)$$

where  $\Psi$  is wave function and  $k$  is wave vector. For the case  $a/2L_x \ll 1$  we use the volume perturbation method to solve the Helmholtz equation<sup>2</sup>. The idea is as follows: The whole volume is divided in two parts, such as the Main Volume (MV) and Additional Volume (AV). The MV is supposed to be much larger than the AV, and it defines the form of solutions for the whole composite volume. Next, solutions of the

composite volume, are searched in the form of solutions of the MV. The method is especially effective in the case where the MV has a simple geometry, for example a rectangular geometry, allowing separation of the variables. In our case, the whole volume in Fig. 1 can be divided in two. We regard the big rectangular box as the MV and the total volume of strips as the AV. Let  $\Psi_m(x, y, z)$  be the wave function of electron in the MV and  $\Psi_a(x, y, z)$  in the AV. The matching conditions will be  $\Psi_m = \Psi_a$ , and an equation of partial derivatives of  $\Psi$  from two sides, for all points of the connection area. Analysis show that maximized spectrum of wave vector  $k$  in RPEB is following <sup>3</sup>:

$$k^x_p = \pi p/a, \quad k^y_q = \pi q/w, \quad k^z_i = \pi i/L_z. \quad (2)$$

Here,  $k^x_p$ ,  $k^y_q$  and  $k^z_i$  are x, y, z components of wave vectors and  $p, q, i=1, 2, 3\dots$ . Eq. 2 indicates the dramatic reduction in spectrum density of x and y components of wave vector, compared to spectrum density of PEB ( $k^x_n = \pi n/L_x, k^y_j = \pi j/L_y, k^z_i = \pi i/L_z$ ).

To extrapolate results obtained for RPEB to low-dimensional metal we use a quantum model of free electrons. For  $T > 0$ , there are two types of free electrons inside the Fermi gas. Electrons with  $k \approx k_F$  interact with their environment and define the transport properties of metals. Electrons with  $k \ll k_F$  do not interact with the environment, because all quantum states nearby (in  $k$  space) are already occupied by other electrons. Such electrons are ballistic and have formally infinite mean free path. This feature allows us to regard them as planar waves, traveling between the walls of the low-dimensional metal. Further, we will concentrate on such ballistic electrons. Once we work with electrons having infinite (or very long) mean free paths, we can regard the low-dimensional metal as a potential-energy box and extrapolate our calculations to it <sup>4</sup>. We found that in metal films with ridged surface, the volume of elementary cell in  $k$  space increase because of QID. Electrical neutrality requires that

the same (normalized to volume) number of electrons occupy separate quantum levels. Therefore Fermi sphere expands and Fermi vector increase to the value  $k_R = k_F [L_y(L_x + a/2)/(aw)]^{1/3}$ . Here  $k_R$  is Fermi vector in ridged film and  $k_F$  is Fermi vector in plain film. For Fermi energy we find

$$E_R = E_F + \alpha_n E_F \{ [L_y(L_x + a/2)/(aw)]^{2/3} - 1 \}, \quad (3)$$

where  $E_R$  and  $E_F$  are Fermi energy of ridged and plain films. In practice, electron de Broglie wave will scatter on irregularities such as grain boundaries inside the film and roughness on the surface. This reduces QID waveband. Corresponding reduction constant  $0 < \alpha_n < 1$  is introduced in Eq.3 to adjust it to particular set of irregularities. For ideal single crystal with zero surface roughness  $\alpha_n = 1$ .

## Sample preparation and experimental results

At NIL Technology ([www.nilt.com](http://www.nilt.com)) substrates were prepared by growing a 50 nm thick thermal oxide on standard 4 inch silicon wafers. The oxide was grown by a dry process at 1000°C. The surface roughness,  $R_a$ , of the oxide surface was measured to be 0.2 nm comparable to the measured roughness of a blank silicon wafer. In order to align the metal pads to the nano-indented areas alignment marks were defined in the oxide film by standard UV-lithography and BHF, 12.5%, etching. The nano-indented areas were defined by 100 kV electron beam lithography, Jeol JBX9300FS, in a 55 nm thick spin coated ZEP520A<sup>5</sup> film developed in ZEP-N50 developer. After development of the ZEP520A any residual resist in the bottom of the nano-indented areas were removed by a low power oxygen plasma with a resist etch rate of 10 nm/min in a resist barrel asher in order to ensure that the thermal oxide got equally

exposed to the BHF in the subsequent transfer of the nano-indented areas into the thermal oxide. The nano-indented areas were transferred into the thermal oxide by a 15 s dip in 4.2% BHF solution using the ZEP520A as the masking material. 15 s dip corresponds to a measured etch depth of approximately 8 nm (measured by AFM, Dimension 3100 from Veeco). After transferring the nano-indented areas into the thermal oxide any remaining ZEP520A was removed by oxygen plasma and the substrates were RCA ( $\text{NH}_4\text{OH}:\text{H}_2\text{O}_2:\text{H}_2\text{O}$  at  $80^\circ\text{C}$  and  $\text{HCl}:\text{H}_2\text{O}_2:\text{H}_2\text{O}$  at  $80^\circ\text{C}$ ) cleaned. Finally the metal pads were defined by standard UV-lithography, electron beam metal evaporation, and lift-off. 30 Å of Ti was deposited as an adhesion layer for 600 Å Au Fig.2. Gold film was deposited on a substrate at room temperature.

At TSU standard 2 inch Si wafers with thermally grown 50 nm dry oxide were used as substrate. After a conventional cleaning procedure, a layer of photoresist S1813 of thickness of 0.6  $\mu\text{m}$  was spun on at 4000 rpm. Interference microscope MII-4 was used for thickness control. Periodic lines 0.8  $\mu\text{m}$  wide were created in the photoresist using UV photolithography, and the  $\text{SiO}_2$  was etched using  $\text{NH}_4\text{F}+\text{HF}+\text{H}_2\text{O}$ , at a rate of 1 nm/ s to a depth of 10–50 nm. In the next step, the photoresist was removed using acetone followed by a conventional cleaning procedure. A further layer of photoresist was attached, and another photolithographic step was used to form large structures using a lift-off process. Metal films of Au, Cr, and Nb were deposited on substrates at vacuum of  $2\text{-}5 \cdot 10^{-6}$  Torr (Fig.2). Au and Cr were evaporated using rapid vacuum evaporation and quench condensing. Nb was deposited using e-beam evaporation. The thickness of the films was 20-100 nm. Substrate temperatures were 245-250 K for Au, 90-140 K for Cr and 90-170 K for Nb. Film growth rates were 20 nm/sec for Au, 1.5 nm/sec for Cr, and 0.3 nm/sec for Nb.

Measurements of the work function were made using the Kelvin probe (KP) method. All measurements were comparative to exclude absolute inaccuracies: the difference between KP readings on a flat region of the film was compared with the reading from the ridged region of the film.

For all samples measured, the ridged regions showed a reduced work function (WF) compared with the plain regions. The magnitude of this reduction of WF,  $\Delta\phi$  depended on the structure of the film and the width of the indents (at fixed indent depth).  $\Delta\phi$  was in the range of 0.15-0.33 eV for Au, 0.3-0.42 eV for Cr and 0.15-0.32 eV for Nb. Metal films (Au, Cr, and Nb) deposited at low temperature substrate always show higher  $\Delta\phi$  than the same films deposited at room temperature. Low temperature deposition reduces mobility of metal atoms on the substrate and results in smaller grain size and more amorphous structure of the film<sup>6,7</sup>. Grain size limits the waveband of QID. Electron could be regarded as localized inside the grain, if its de Broglie wavelength is less than grain diameter  $d$ . In the case  $\lambda > d$ , free electron belongs to all granolas simultaneously. For electrons with  $\lambda > d$ , boundary conditions are defined by the indented geometry of the film, while for electrons with  $\lambda < d$  boundary conditions are defined by the particular grain. Therefore, grain size defines the critical de Broglie wavelength  $\lambda_c = d$ , below which QID is suppressed. Consequently QID waveband depends on grain size which itself depends on the temperature of the substrate and film growth rate. Experiments show higher value of QID, for films with smaller grain size (lower substrate temperature). This is in agreement with theory.

In order to measure dependence of  $\Delta\phi$  on indent width  $w$ , samples containing areas with different  $w$  were prepared on the same substrate. Wafers with ridged SiO<sub>2</sub> layer having indent depth of  $a=8$  nm were prepared in NILT. Indent width was in the

range of  $w=0.2-3 \mu\text{m}$ . Au film was e-beam deposited at room temperature substrate at NILT. Another Au film was deposited on the same substrate in TSU using rapid thermal evaporation and quench condensing at  $T=245 \text{ K}$ . Dependences  $\Delta\phi(w)$  for both NILT and TSU films are shown on Fig. 3. Both dependences exhibit diffuse peak around an indent width of  $0.7 \mu\text{m}$ . TSU films grown on cold substrate show greater reduction in WF. No peak was observed in  $\Delta\phi(w)$  for Cr films deposited on the same substrate. Increase of  $\Delta\phi(w)$  was observed in Cr films below  $0.4 \mu\text{m}$ . Our explanation of peak in Au films is following. Electron energy distribution in granular films, strongly deviate from Fermi function. Particularly there is large peak at energies 5-6 eV below Fermi level in electron energy distribution of Au films<sup>8</sup>. When indent width  $w$  matches de Broglie wavelength of those electrons forming peak in energy distribution, QID effect influence the peak region and causes most reduction in WF. In another words quantum states become forbidden in energy region where large number of electrons are concentrated, resulting in more increase of Fermi level and corresponding reduction in WF.

Dependence of WF reduction on indent depth  $\Delta\phi(a)$  was studied in our previous experiments<sup>9</sup> and also show qualitative agreement with the theory.

## Conclusions

We show that, in the low-dimensional metal films with ridged surface, QID effect reduce the energy spectrum density for electrons and increase the Fermi energy. Using volume perturbation method we calculate approximate analytical expression for the relative increase of the Fermi energy. Our resent experiments show reduction of work function in Au, Nb, Cr and  $\text{SiO}_2$  thin films with ridged surface. Degree of QID depends on the structure of the film. For quench condensed films we always measure

more work function reduction. Our interpretation is that QID is effective only in the narrow waveband of de Broglie waves, having wavelength more than grain diameter. Dependence of work function reduction on indent width was measured for Au and Cr films. Obtained dependences could be explained in terms of electron energy distribution function in particular material. Experimental results are in qualitative agreement with QID theory. To achieve qualitative agreement we introduce coefficient, describing irregularities, into the formula for Fermi energy of ridged films. It is expected that QID effect will be much more pronounced in single crystals. Possible candidates are Silicon on insulator SOI wafers having thin layer of single crystal with almost ideal structure attached to insulator substrate. Reduction of the work function of the thin films will have practical use for devices working on the basis of electron emission and electron tunneling. In addition, such layers will be useful in the semiconductor industry, particularly for the structures in which contact potential difference between two layers plays an important role.

## **Acknowledgments**

Work is financed and supported by Borealis Technical Limited, assignee of corresponding U.S. patents (7,166,786; 7,074,498; 6,281,514; 6,495,843; 6,680,214; 6,531,703; and 6,117,344).

### References:

1. Yao J-C Woo, ed., *Physics and Applications of Semiconductor Quantum Structures* (IOP, Bristol, 2001).
2. V.M. Sedykh, *Waveguides With Cross Section of Complicated Shape* (Kharkhov University press, 1979), p.16; William S. C. Chang, *Principles of Lasers and Optics* (University of California, San Diego, 2005).
3. A. Tavkheldze, V. Svanidze, and I. Noselidze *J. Vac. Sci. Technol. B*, v. 25(4), (2007).
4. V.V. Pogosov, V.P. Kurbatsky, and E.V. Vasyutin, *Phys. Rev. B*, **71**, 195410 (2005).
5. Zeon corporation Tokyo Japan [www.zeon.co.jp](http://www.zeon.co.jp)
6. K. L. Ekinci and J. M. Vallers Jr. *Acta mater.* Vol. 46, No. 13, p. 4549, (1998).
7. N.G. Semaltianos, E.G. Wilson *Thin Solid Films* 366, p. 111, (2000).
8. T.K. Sham, P.-S.G. Kim, P. Zhang *Solid State Communications* 138 p.553, (2006).
9. A. Tavkheldze *et al.*, *J. Vac. Sci. Technol. B* **24**, 1413 (2006).

### **Figure Captions:**

**Fig. 1. 3D view of indented potential-energy box. Dash line depicts border of Main volume and additional volume.**

**Fig.2. Metal film having ridged surface grown on Si/SiO<sub>2</sub> substrate.**

**Fig. 3. Work function reduction dependence on indent width. Circles - NILT grown films and triangles - TSU grown films.**

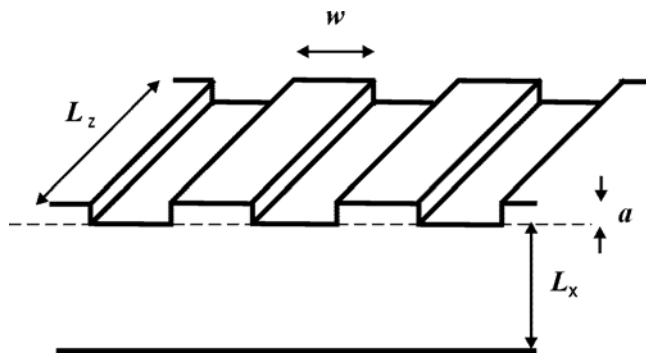


Fig.1

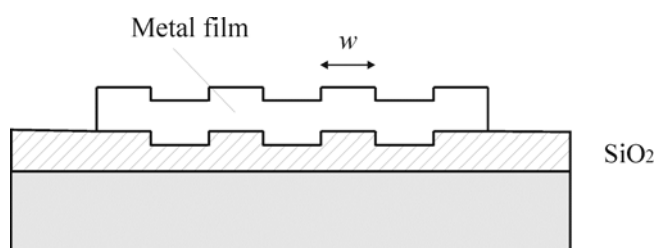


Fig.2

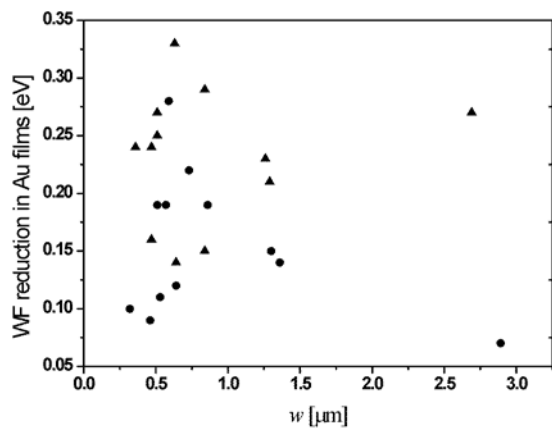


Fig. 3.

**Material terms: Au, Nb, Cr**

**Corresponding author: Avto Tavkhelidze**

**Address:**

Dr. Avto Tavkhelidze  
Microelectronics Department  
Tbilisi State University  
Chavchavadze Ave. 13  
0179 Tbilisi  
Georgia Republic

**Tel:** +995 99 58 73 16

**Fax:** +995 32 22 73 95

**E-mail:** [avtotav@geo.net.ge](mailto:avtotav@geo.net.ge)